

Drops impacting a sieve

Élise Lorenceau and David Quéré*

Laboratoire de Physique de la Matière Condensée, UMR 7125 du CNRS, Collège de France, 75231 Paris cedex 05, France

Received 23 September 2002; accepted 31 January 2003

Abstract

We study experimentally the impact of liquid drops against thin plates pierced with small holes. When the drop is larger than the hole, different situations can occur: (i) at a small velocity, the drop is entirely captured by the plate; (ii) above a threshold speed, some liquid is ejected below the surface. We characterize this critical speed and these two different situations, focusing on the forces able to slow down the drop. We also quantify the amount of liquid ejected out of the hole.

© 2003 Elsevier Science (USA). All rights reserved.

Keywords: Impact; Wetting; Filtration

1. Introduction

Many industrial and environmental processes involve the impact of drops on solid surfaces (ink jet printing, pesticide spraying, atomizing). This subject has thus been extensively studied, but because of its complexity, most analyses have done been assuming quite ideal cases, i.e., pure liquids on smooth planar surfaces [1]. More complex cases have been investigated recently. For example, Rozhkov et al. were interested in the impact of drops against small circular targets [2]. In the present work, we consider the complementary case of a drop impacting a hole, smaller than the drop and than the capillary length. Thus, a drop gently deposited on the hole cannot pass through it because of surface tension (and we shall neglect gravity as a possible cause of crossing the plate), but of course can do it if violently thrown, because of its inertia. Our main aim here is to analyze both the threshold in velocity above which some liquid passes through the hole and to determine the quantity which comes out above this threshold. This is the first step for understanding the trapping of aerosols through grids or filters, which consist of holes and solids—in order to capture the liquid phase, but let the gaseous one permeate. Similar grids can be used for recovering water from morning fog in deserted areas, or to reduce the noxious emission of liquid aerosols by chemical plants.

2. Observations

A free-falling drop of liquid impacting a surface pierced with a single hole is observed using a high-speed camera, with typically 1000 frames per second (Fig. 1). Drop diameters D are in the range of 1.5–3 mm, and their velocities V vary from 0 to 3 m/s. The surface is stainless steel 0.25 mm thick, with holes of radius r in the range 0.13–0.45 mm. The axis of symmetry of the hole coincides with the drop trajectory. We use different liquids (generally wetting the solid), of viscosities η varying from 0.5 to 500 mPa s.

Figure 2 shows a sequence obtained with a drop of silicone oil ($\eta = 0.5$ mPa s) impacting at a velocity of 50 cm/s a stain plate pierced with a hole about five times smaller than the drop. It is observed that for such a small velocity, all the liquid finally remains on the surface: the

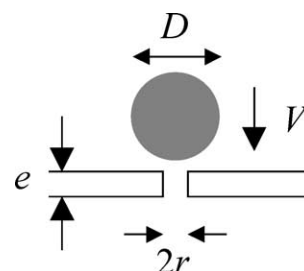


Fig. 1. Liquid drop impacting a solid surface pierced with a small hole.

* Corresponding author.

E-mail address: david.quere@college-de-france.fr (D. Quéré).



Fig. 2. Set of pictures taken each 2 ms ($D = 3.5$ mm, $r = 390$ μm , $V = 50$ cm/s). The drop (silicone oil of surface tension $\gamma = 16$ mN/m and viscosity $\eta = 0.5$ mPa s) is entirely captured by the surface. The hole is in the middle of each frame. Below it, a liquid finger transiently forms and retracts; above it, we see in the pictures both the impacting drop and the reflection of the finger.

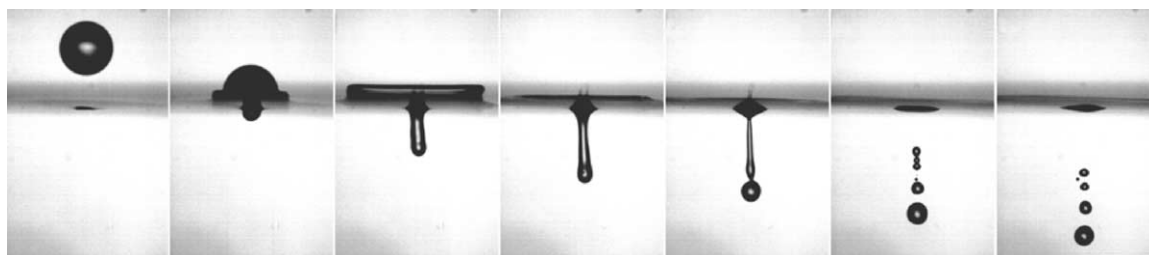


Fig. 3. Set of pictures taken each 2 ms ($D = 3.5$ mm, $r = 450$ μm , $V = 70$ cm/s). Liquid (same silicone oil as in Fig. 2) is ejected from the surface and turns into several drops.

capture of the drop is total. Note that a liquid finger transiently forms below the hole, before finally retracting.

For the same drop impacting at a higher velocity ($V = 70$ cm/s), some liquid is ejected below the hole, and only a small fraction remains captured, as can be observed in Fig. 3. The threshold for liquid ejection (denoted as V^*) is well defined and can easily be measured experimentally, either with high-speed photographs or even more simply by placing a wetting surface beneath the hole and looking to see if it is wetted by the ejected liquid.

3. Critical velocity of crossing

In this problem, the liquid inertia tends to make the drop cross the hole, while two forces are antagonist: on one hand, the viscous friction related to the crossing of the hole, and on the other hand, capillary forces which oppose the formation of a liquid finger. To highlight the contribution of these two forces, the natural parameters to consider are the Reynolds number Re and the Weber number We , which compare inertia with viscosity and capillarity, respectively. We consider in particular these two numbers at the threshold velocity V^* ,

$$Re^* = \frac{\rho V^* r}{\eta},$$

$$We^* = \frac{\rho V^{*2} r}{\gamma},$$

where the radius of the hole r was taken as a characteristic length. Both these numbers can be determined experimentally, and we report in Fig. 4 the variation of We^* as a function of Re^* for various liquids and hole radii.

In the limit of small Re , the viscous force is dominant and should be responsible for the capture of the drop: this leads to a vertical asymptote $Re^* \approx 5$ in Fig. 4. For intermediate

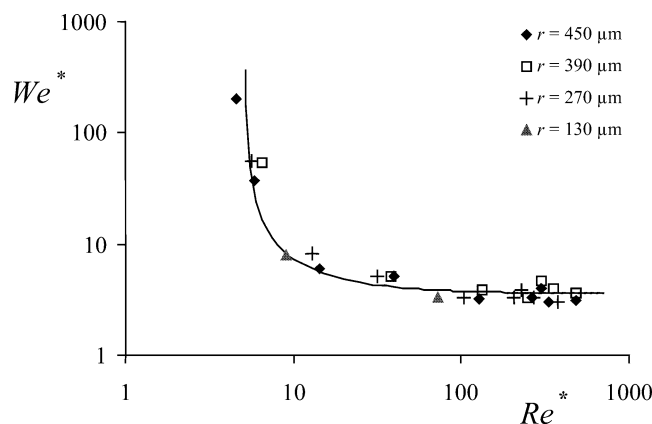


Fig. 4. Threshold velocity of capture: the Weber number at the threshold is plotted as a function of the Reynolds number at the threshold. The data are obtained using a 250- μm -thick plate, different hole radii, and various liquids (silicone oils of viscosity ranging between 0.5 and 300 mPa s, ethanol, acetone, heptane, and water). The thin line is the curve $Re^* - 3.6 = 5.1 We^*$, where the scaling comes from Eq. (1).

Re ($5 < Re < 100$), the two numbers are observed to depend on each other. Both the capillary and the viscous forces play a role. At large Re ($Re > 100$), the critical Weber number is found to be constant, of about 3.5: the critical speed does not depend on viscosity and is set by a balance between inertia and capillarity. We call this regime *capillary–inertial*.

In the limit of very thin plates ($e < r$), the viscous force associated with the crossing of the hole can be dimensionally written $\eta V r$ (the velocity gradients taking place on a size of order r). The capillary force opposing the formation of a liquid finger scales as γr . Balancing these two forces with inertia gives an equation for the threshold: $\rho V^{*2} r^2 \sim \eta V^* r + \gamma r$. This yields

$$Re^* \sim \frac{We^*}{We^* - 1}, \quad (1)$$

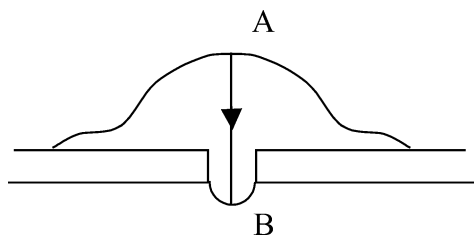


Fig. 5. Drop of diameter D impacting a surface with a hole. In A, the curvature and speed are of order $1/D$ and V , while they are of order $1/r$ and 0 in B.

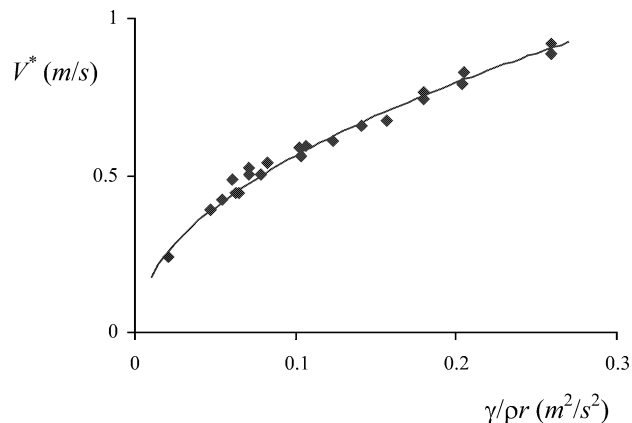


Fig. 6. Critical speed of capture, as a function of the ratio $\gamma/\rho r$. Liquids used are ethanol, acetone, and silicon oil. The straight line is a power law fit of exponent 0.495 and prefactor 1.8.

where all the numerical coefficients have been ignored. An equation of the type (1) is indeed found to describe fairly well the data in Fig. 4, where the equation $Re^* (We^* - 3.6) = 5.1We^*$ is represented with a thin line.

We now discuss more precisely the capillary–inertial regime. The threshold velocity is given by a balance between the dynamic pressure $1/2\rho V^{*2}$ and the Laplace pressure in the finger $2\gamma/r$ (point B in Fig. 5), neglecting the Laplace pressure in the drop, taken larger than the hole.

Hence, we get for the critical speed

$$V^* = 2\sqrt{\frac{\gamma}{\rho r}}. \quad (2)$$

We report in Fig. 6 the critical speed measured for different liquids and hole radii, as a function of the quantity $\gamma/\rho r$, in the capillary–inertial regime. The straight line corresponds to a power law of exponent 0.495, with a coefficient of 1.78, both in good agreement with Eq. (2).

It is worth noting that the ratio $\sqrt{\gamma/\rho r}$ is proportional to the speed of retraction of a free edge bounding a sheet of uniform thickness r , as shown by Taylor [3]. Taylor's calculation can be extended to the geometry of a cylinder of radius r [4]. The surface tension acts on the edge, in order to reduce the length of the cylinder, with a force $2\pi r\gamma$. Balancing this force with the derivative of the momentum dMV/dt (where M and V are the mass and velocity of the edge), we obtain a constant velocity of retraction similar to

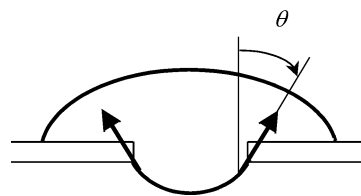


Fig. 7. Onset of finger formation. The arrows indicate the direction of the capillary force.

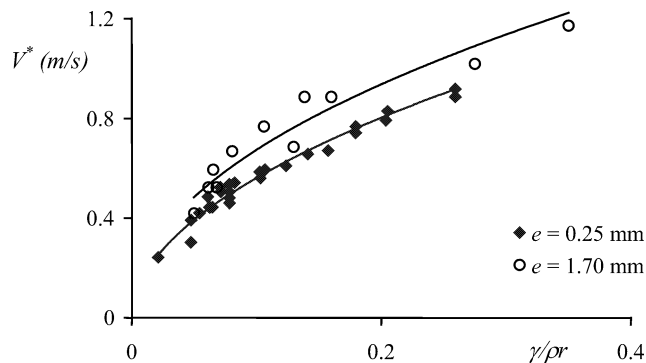


Fig. 8. Critical speed of capture as a function of the ratio $\gamma/\rho r$ for different plate thicknesses. The thickness is either 1.7 mm (open circles) or 0.25 mm (full diamonds).

the one given by Eq. (1), but with a different prefactor ($\sqrt{2}$ instead of 2). This discrepancy between the results given by a force balance and by the conservation of energy (as implicitly assumed in Eq. (1)) is a common feature of all kind of retraction problems, in the inertial limit (bursting of a soap film, fast dewetting, inertial capillary rise, etc.) [5–8]. But our main conclusion remains: liquid can be ejected from the hole only if the drop velocity is larger than the retraction velocity of the cylindrical jet, which defines a threshold of ejection scaling as $\sqrt{\gamma/\rho r}$, as observed experimentally. For the numerical coefficient, the data displayed in Fig. 6 provide 1.78, a value intermediate between $\sqrt{2}$ and 2.

Note that we observe in Fig. 2 a finger forming below the threshold velocity. This can be due to the fact that at the beginning of the finger formation, the surface tension forces not only pull in the vertical direction, but also in the horizontal one (Fig. 7).

This gives as a capillary force in the vertical direction $2\pi r\gamma \cos\theta$, denoting as θ the angle between the liquid/air interface and the vertical direction. This force is smaller than assumed above, which can explain that a finger (transiently) forms, even below the threshold V^* .

In the same capillary–inertial regime, we finally tested the influence of the thickness e of the surface using two plates of respective thickness 0.25 mm and 1.7 mm. Figure 8 shows the critical speed as a function of the ratio $\gamma/\rho r$ for the two surfaces.

The threshold of capture is weakly affected by the plate thickness (although both plates have quite different thicknesses): both laws remain parabolic (exponent 0.495 for the thick plate, and 0.47 for the thin one), with comparable numerical coefficients (1.78 ± 0.10 and 2.02 ± 0.15 , respec-

tively). But it is observed that the critical speed is slightly higher for the thicker plate, which could be due to an additional viscous dissipation along the hole.

4. Above the critical speed

We finally consider the case of a drop impacting the surface with a speed larger than the critical speed, as in Fig. 3. Drops are ejected from the surface, and we try to characterize their formation. Figure 3 suggests that they just come from the destabilization of the liquid column (Plateau–Rayleigh instability). We measured t^* the time for pinching off, which is reported in Fig. 9 as a function of the speed of impact, for different hole radii.

The time of pinch-off is found to be quite independent of the speed of impact, but it strongly depends on the radius of the hole. The average value of this time is 7.2 ms for the hole of radius 390 μm , 3.8 ms for the 270- μm one, and 1.6 ms for the 130- μm one. It thus increases with r , in qualitative agreement with Plateau–Rayleigh instability. For a liquid column of small viscosity, the destabilization takes place in a time t_R obtained by balancing inertia (of the order of $\rho r/t_R^2$) with capillarity (of the order of γ/r^2), which yields [9]

$$t_R \sim \sqrt{\frac{\rho r^3}{\gamma}}. \quad (3)$$

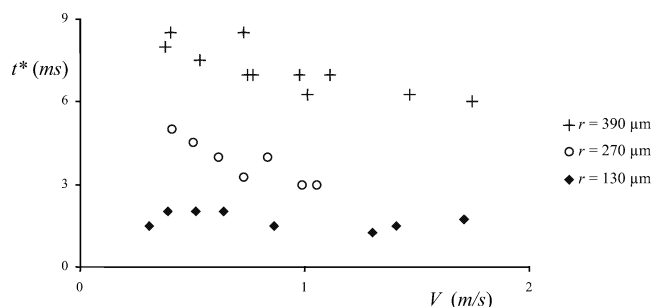


Fig. 9. Time of pinch off as a function of the speed of impact for three different hole radii.

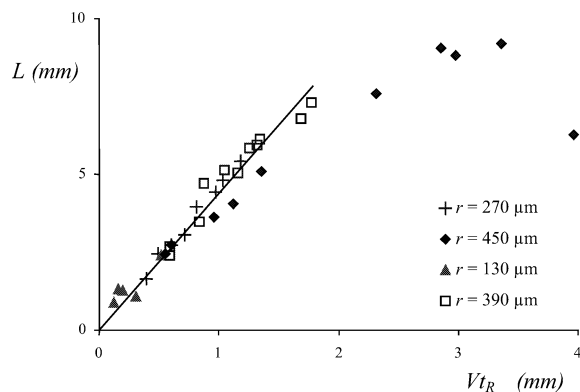


Fig. 10. The maximal length of the cylinder versus the product of the speed with the Rayleigh time. All the results fit on the same straight line (of slope about 4).

Thus t_R increases as $r^{3/2}$ and does not depend on the speed of impact V . Nevertheless, our experiment cannot provide any precise information: (i) the highest speed rate of the camera is 1 ms, of order t_R for the smallest cylinder; (ii) the data are obtained only with three radii. Yet much more quantitative data could be obtained by measuring the maximal length of the cylinder.

Figure 10 displays the maximal length L of the cylinder before it breaks down, as a function of the length on which the Plateau–Rayleigh instability should take place, namely the quantity Vt_R (supposing that the velocity of the jet remains of the order of the impact velocity V). It is observed that the maximal size of the cylinder increases linearly with the length Vt_R (with a slope of the order of 4), before slowing down for large lengths, for which the flow is not laminar (see Fig. 11). Moreover, all the data (even those obtained using different hole radii) fit on the same curve. Figure 10 thus confirms the assumption made using Fig. 9: as long as the cylinder has not broken, it keeps on growing at a speed V , which provides as a maximal length the product Vt_R . In addition, the proportionality between L and Vt_R provides information on the speed of the jet V_j in the regime where the speed of impact is higher than the critical speed V^* . L is indeed defined by the equation

$$L = \int_0^{t_R} V_j dt \sim V_j t_R.$$

Since we get experimentally $L \sim Vt_R$, we deduce that $V \sim V_j$. Note that when the saturation occurs in Fig. 10, i.e., for a very large impact speed, the jet appears qualitatively different, as can be observed in Fig. 11. In particular, the liquid ejected from the hole is twisted, showing that the flow is not laminar.

The number of drops ejected from the surface can finally be estimated, thanks to the experimental result of Fig. 10. As stressed above, a long cylinder of liquid is unstable: when its perimeter is larger than $2\pi r$, it turns into two drops (neglecting the possible emission of satellite droplets). For an infinite column, the wavelength of the instability (which is selected kinetically), is slightly larger than $2\pi r$, but remains of the same order [9]. Hence, we get as a

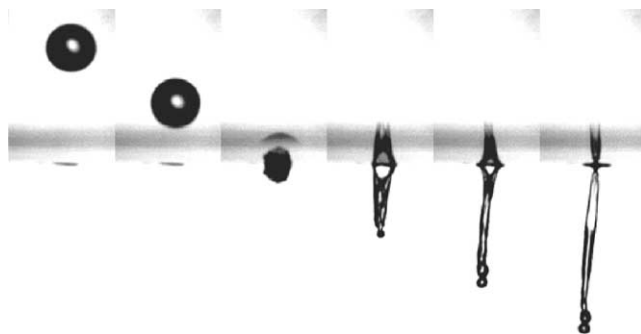


Fig. 11. Impact of a high-speed drop ($V = 2$ m/s) into a hole of radius 450 μm .

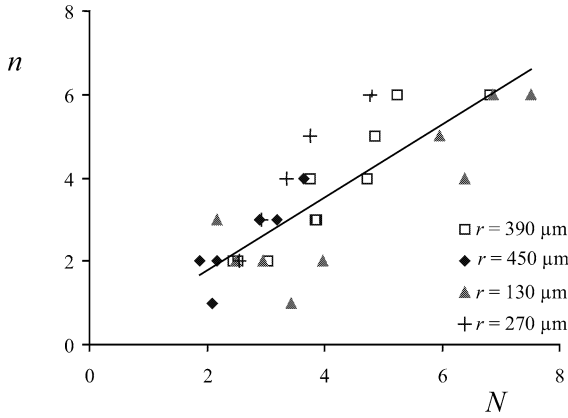


Fig. 12. Number of drops ejected below the hole, as a function of the number calculated using Eq. (3), for four different hole radii.

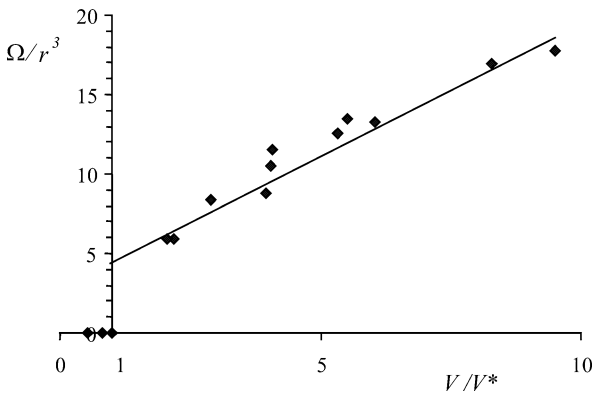


Fig. 13. Volume of liquid ejected from the hole over the radius of the hole to the power of three vs the speed over the critical speed for different radii.

theoretical number of ejected droplets

$$N \approx \frac{L}{2\pi r} + 1.$$

With $L \sim 4Vt_R$, we deduce

$$N \approx \frac{4V}{2\pi V^*} + 1. \tag{4}$$

Figure 12 shows the observed number n of ejected drops as a function of N , the number given by Eq. (4), for different hole radii.

The observed behavior is in qualitative agreement with Eq. (4) (the full line indicated a slope of 0.9) in spite of discretization of both axes. This simple analysis thus allows us to determine the number of ejected drops, which is a parameter of practical importance.

This can be complemented by the question of the volume Ω of liquid ejected. We expect it to be of the order of r^2L , and thus scaling as r^2Vt_R (from Fig. 10). Using Eq. (3), this volume can be written

$$\Omega \sim r^2 V \sqrt{\frac{\rho r^3}{\gamma}},$$

which is extremely sensitive to the hole radius (variation in $r^{7/2}$). Using the proper scaling for V^* (Eq. (1)), we finally deduce

$$\Omega \sim \left(\frac{V}{V^*}\right) r^3. \tag{5}$$

Our different data are reported in Fig. 13, where they are compared with Eq. (5). We plot the ejected volume (normalized by r^3) as a function of the impact velocity (normalized by the threshold velocity V^*), as suggested by Eq. (5).

It is observed that all the data fit on the same line, which intercepts the y-axis for Ω/r^3 of about 4. Hence, when the speed of the drop is just above the critical speed, the ejected volume is about $4\pi/3r^3$ and there is nothing below the hole but one single drop shaped by the hole, as can be observed in Fig. 14. Most of the impacting liquid is captured by the plate (typically 80% in the example of Fig. 14) and remains trapped in the hole. Note also the slight slowing down of the drop due to the formation of a wetting meniscus above the drop to be ejected, which opposes its detachment.

5. Conclusion

We studied here the impact of a drop onto a solid plate pierced by a small hole. Above a threshold velocity, droplets were observed to be ejected out of the hole. We showed that for liquids of low viscosity (Reynolds number larger than 100), the threshold is fixed by a balance between capillarity and inertia and thus scales as $\sqrt{\gamma/\rho r}$. Together with the condition of high Reynolds number, this result implies that this regime is limited to liquids of viscosity smaller than $\sqrt{\gamma\rho r}$. For larger viscosities, the threshold velocity of ejection was found to increase rapidly (Fig. 4) and shown to result from a balance between viscous friction and inertia.

In the capillary–inertial regime, and above the threshold velocity, we also studied the dynamics of the liquid cylinder ejected out the surface and described the mechanism of its transformation into droplets. Thanks to scaling arguments,

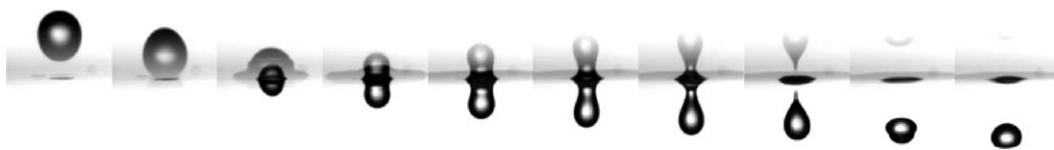


Fig. 14. Set of pictures taken each 2 ms showing the ejection of one single drop of diameter about the hole size ($r = 390 \mu\text{m}$). The experiment is done with a drop ($D = 3.5 \text{ mm}$) of a light silicone oil ($\gamma = 16 \text{ mN/m}$ and viscosity $\eta = 0.5 \text{ mPa s}$) impacting the pierced plate at a velocity $V = 40 \text{ cm/s}$, just above the threshold V^* .

we could propose a first-order analysis allowing us to predict the volume of the liquid cylinder and the number of ejected droplets. In particular, it was shown that close to the threshold, single calibrated droplets are shaped by the hole.

Acknowledgment

It is a pleasure to thank Christophe Clanet for very helpful discussions.

References

- [1] M. Rein, *Fluid Dynam. Res.* 12 (1993) 61.
- [2] A. Rozhkov, B. Prunet-Foch, M. Vignes-Adler, *Phys. Fluids* 14 (2002) 3485.
- [3] G.I. Taylor, *Proc. Roy. Soc. London Ser. A* 259 (1960) 1.
- [4] C. Clanet, J.C. Lasheras, *J. Fluid. Mech.* 383 (1999) 307.
- [5] F.E.C. Culick, *J. Appl. Phys.* 31 (1960) 1128.
- [6] A. Buguin, L. Vovelle, F. Brochard-Wyart, *Phys. Rev. Lett.* 83 (1999) 1183.
- [7] D. Quéré, É. Raphaël, J.Y. Ollitrault, *Langmuir* 15 (1999) 3679.
- [8] P.G. De Gennes, *Faraday Discuss.* 104 (1996) 1.
- [9] Lord Rayleigh, *Philos. Mag.* 34 (1892) 145.